論文 / 著書情報
Article / Book Information

Title	Low friction of nitrogen-doped diamond-like carbon coating due to acidic liquid film and nitrogen-doped graphite oxide generated by dielectric barrier discharge in ambient air
Authors	Wenjun Wu, Motoyuki Murashima, Noritsugu Umehara, Takayuki Tokoroyama, Ruixi Zhang
Citation	Surfaces and Interfaces, Vol. 56, No. 105591, pp. 1-10
Pub. date	2025, 1
DOI	https://dx.doi.org/10.1016/j.surfin.2024.105591
Creative Commons	Information is in the article.

Surfaces and Interfaces 56 (2025) 105591

Contents lists available at ScienceDirect

Surfaces and Interfaces

journal homepage: www.sciencedirect.com/journal/surfaces-and-interfaces

Low friction of nitrogen-doped diamond-like carbon coating due to acidic liquid film and nitrogen-doped graphite oxide generated by dielectric barrier discharge in ambient air

Wenjun Wu [a,*], Motoyuki Murashima [b,*], Noritsugu Umehara [a], Takayuki Tokoroyama [a], Ruixi Zhang [a]

[a] Department of Micro-Nano Mechanical Science and Engineering, Nagoya University, Furo-cho, Chikusa-ku, Nagoya, Aichi 464-8603, Japan

[b] Department of Mechanical Systems Engineering, Tohoku University, 6-6-01 Aoba, Aramaki, Aoba-ku, Sendai, Miyagi 980-8579, Japan

ARTICLE INFO

Keywords:
Nitrogen-doped diamond-like carbon coating (*ta-CN*$_x$)
Dielectric barrier discharge (DBD)
Liquid film
Nitrogen-doped graphite oxide
Low friction

ABSTRACT

This study investigated the low friction mechanism of nitrogen-doped tetrahedral amorphous carbon (*ta*-CN_x) coatings using *in-situ* irradiation of dielectric barrier discharge (DBD) in ambient air. When the *ta*-CN_x surface was irradiated with DBD, an acidic liquid film was produced, which was analyzed using liquid chromatography-mass spectrometry (LC/MS) to show that the liquid film contained nitric acid. Additionally, DBD-irradiated surfaces and wear track of low-friction surfaces (surface with friction coefficient reduced to 0.01) were analyzed using Raman, XAFS, and XPS, and the results consistently showed that DBD irradiation produced nitrogen-doped graphite oxide (N-GO) structures. The study conclusively demonstrated that the synergistic effect of the N-GO and the acidic liquid film is crucial for achieving low friction, with each component being indispensable for the effectiveness of the mechanism. This synergy highlights the potential of DBD irradiation as a novel approach for enhancing lubrication in *ta*-CN_x coatings.

1. Introduction

The OECD's 2014 bulletin states that 38 % of the key technologies for lowering CO_2 emissions are related to end-use energy efficiency [1], and tribology research is included in this group. Furthermore, a significant amount of the yearly CO_2 emissions worldwide are caused by wear and friction [2]. As a solid lubricant, diamond-like carbon (DLC) is an intriguing material. Because of its bonding structures, its hybridization of sp^2 and sp^3 offers anti-friction and wear-resistance properties [3]. DLC has been widely used as a protective coating in automotive parts, biomedical and optical fields.

Non-hydrogenated amorphous carbon coatings and hydrogenated amorphous carbon coatings are the two categories of DLC coatings. The presence of hydrogen in DLC:H coatings help terminate the dangling carbon bonds. This termination reduces the reactivity of the surface, thereby reducing friction. Erdemir shows that highly hydrogenated DLC exhibits ultra-low friction in dry inert gases and suggests that eliminating strong carbon-carbon interactions through hydrogen termination facilitates the realization of ultra-low friction in DLC [4,5].

However, DLC coatings face certain limitations, including high intrinsic stress, which results in inadequate adhesion [6,7]. In some cases, it is clarified that oxidation degrades the coating morphology [8]. Therefore, the characteristics of DLC coatings may be effectively enhanced by incorporating additional elements, including Si, Ti, N, and Ti/Al co-doping [9–12]. According to reports, N doping, particularly with high nitrogen concentrations, may diminish hardness and decrease sp^3 content. On the other hand, adhesion's tribological characteristics have greatly enhanced [7]. Liu et al. have shown that atmospheric humidity and oxygen significantly influence the characteristics of *ta*-CN_x coatings [12].

Graphene-family materials have a lot of potential for use in tribology. Reviews by Liu et al. offer a thorough analysis of the lubrication mechanisms, potential applications, and challenges of Graphene-family materials, emphasizing their effectiveness in reducing friction and wear in various tribological systems [13,14]. It was also demonstrated that adding graphene-family compounds to water-based lubricants may greatly enhance the tribological characteristics of DLC coatings. Recent research has reported improved DLC tribological

* Corresponding authors.
E-mail addresses: wuwenjun@ume.mech.nagoya-u.ac.jp (W. Wu), motoyuki.murashima.b3@tohoku.ac.jp (M. Murashima).

https://doi.org/10.1016/j.surfin.2024.105591
Received 12 July 2024; Received in revised form 4 December 2024; Accepted 5 December 2024
Available online 6 December 2024

properties, biocompatibility, and mechanical properties through surface modification. Common methods of surface modification include plasma irradiation [15–21], laser or UV irradiation [22,23], and acid modification [24]. Among them, plasma irradiation is widely studied and used. Plasma irradiation modification technology, through plasma treatment, achieves targeted control of material surface properties, offering advantages such as environmental compatibility, high processing efficiency, broad material applicability, and precise controllability. This technique effectively introduces surface functional groups without altering the material's bulk properties, enhancing hydrophilicity, adhesion, and biocompatibility. Kim et al. showed that using oxygen plasma irradiation can reduce the running-in cycles and friction coefficient [25]. Lazauskas et al. discovered that oxygen plasma irradiation enhanced DLC surface hydrophilicity [26]. In recent years, surface modification by plasma irradiation in atmospheric environments has received more attention. Dielectric barrier discharge (DBD) is one of them. DBD is a non-thermal plasma technique that effectively induces cross-linking on the surface of a material, introducing chemical functional groups and active substances [27,28]. Studies have shown that DBD irradiation increases surface energy and wettability [29,30]. In the study, the ability of the *in-situ* surface modification was unveiled, which can follow the active tribological control technology recently developed using an electric field, morphing surface, and AI technology [31–35]. In a previous study, a surface treatment technique using DBD for DLC coatings was developed [36]. The results showed that DBD irradiation caused the friction coefficient decrease to 0.02–0.008. Additionally, previous research has demonstrated the effectiveness of DBD in reducing the friction coefficient of *ta*-CN_x coatings by inducing the formation of a liquid film and a soft material layer on the surface [37]. However, while this study provided valuable insights into the effects of DBD treatment, it did not delve into the composition of the liquid film, the structure of the soft material, or the underlying mechanisms driving the observed low friction.

This study investigates the low friction mechanism of DBD irradiated *ta*-CN_x coating. First, the composition of the acidic liquid film formed by DBD irradiation was analyzed using LC/MS. Secondly, the transformation of the surface structure of DBD irradiated *ta*-CN_x surfaces and wear track was demonstrated. Finally, an explanation of the low friction mechanism was provided.

2. Experimental

2.1. Deposition of ta-CN_x coatings

In this study, the *ta*-CN_x coatings were deposited using the system shown in Fig. 1. The deposition system consists of two parts, including the anode-layer ion source (ALIS) and filtered cathodic vacuum arc (FCVA). The substrate was a SUJ2 disc (22.5 mm diameter, 4 mm thickness). The initial step involved the ultrasonic cleaning of the substrate with benzene and acetone. Subsequently, residual impurities were eliminated by Ar^+ plasma etching. Finally, the hybrid system was used to deposit the *ta*-CN_x coatings. A carbon target (99.99 % purity, TOYO TANSO, Japan) served as the cathode in the vacuum arc source. Carbon ions were accelerated by a substrate bias of −50 V during an arc discharge on the carbon target at a current of 50 A. The deposition procedure took 30 min, and the nitrogen flow rate was 20 sccm. Consequently, a *ta*-CN_x coating was produced with a hardness of 18.1 GPa and a surface roughness of Ra = 5 nm.

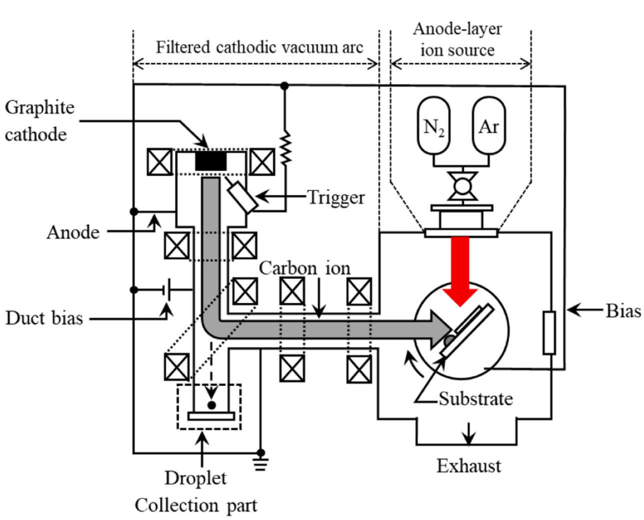

Fig. 1. Schematic of hybrid coating system equipped with ALIS and FCVA.

2.2. Characterization

A ball-on-disk tribometer was used to evaluate the tribological behavior under DBD irradiation (Fig. 2). The friction tests were performed using silicon nitride balls (Si_3N_4, 8 mm diameter) with a load of 0.98 N and a sliding speed of 38 mm/s. Fig. 2b shows the DBD part. A high-frequency power supply (PSI-PG1040F, PSI, Japan) was connected to one end of a cylindrical aluminum electrode, and the other end of the electrode had been covered in a glass sheet of about 150 mm in thickness to act as a dielectric to prevent arc discharge or spark discharge. Another wire from the high-frequency power supply was connected to the bottom of the rotary table, and the disk coated with *ta*-CN_x coating was placed on the rotary table. Finally, an alternating high voltage of 3.5 kV at 4.0 kHz was applied. The gap between the glass sheet and the disk was 350 mm. Upon application of the high-frequency voltage, a DBD was generated. Every test was carried out at room temperature with a 35–40 % relative humidity.

Liquid chromatography-mass spectrometry (LC/MS) was used to evaluate the liquid films produced by DBD irradiation. After friction and discharge tests, the surfaces of the disks and balls were inspected using confocal laser scanning microscopy (Olympus OLS5100, Japan). The surface morphology was characterized by field-emission scanning electron microscopy (FE-SEM, SU-8230, Hitachi High-Tech Corporation, Japan). X-ray photoelectron spectroscopy (XPS, PHI Quantes, ULVAC-PHI, Inc., Japan) was used to determine chemical composition and structure. XPS was performed by radiating Al Kα-excited photons with an energy of 1486.6 eV. The carbonaceous structures were analyzed using a laser Raman spectrometer (RENISHAW inVia Reflex, UK) at a 532 nm wavelength. The measured Raman spectra were fitted to the D peak (1350 cm^{-1}) and G peak (1580 cm^{-1}) wavelength centers using a Gaussian fitting function.

3. Results and discussion

3.1. LC/MS results of liquid film

In the previous study, it was found that DBD irradiation generated a strongly acidic (pH = 2) liquid film [36], so the liquid film generated by DBD irradiation was collected and analyzed using LC/MS. Fig. 3 shows the results of LC/MS analysis. The figure shows that a strong peak appears at the position with a mass of 62, which is NO_3^-. From the result, it can be determined that the liquid film generated by DBD irradiation contains rich nitric acid. Here, it is important to note that nitric acid, as a potent oxidizing agent, usually oxidizes graphite [38].

3.2. Friction coefficient during in situ DBD irradiation

The evolution of the friction coefficient of the *ta*-CN_x coating during DBD irradiation is shown in Fig. 4. First, a friction test was conducted, and sliding stopped immediately when the friction coefficient dropped below 0.02. As seen in Fig. 4a, the friction coefficient was reduced to 0.01 after the third DBD irradiation, and the friction test was ceased

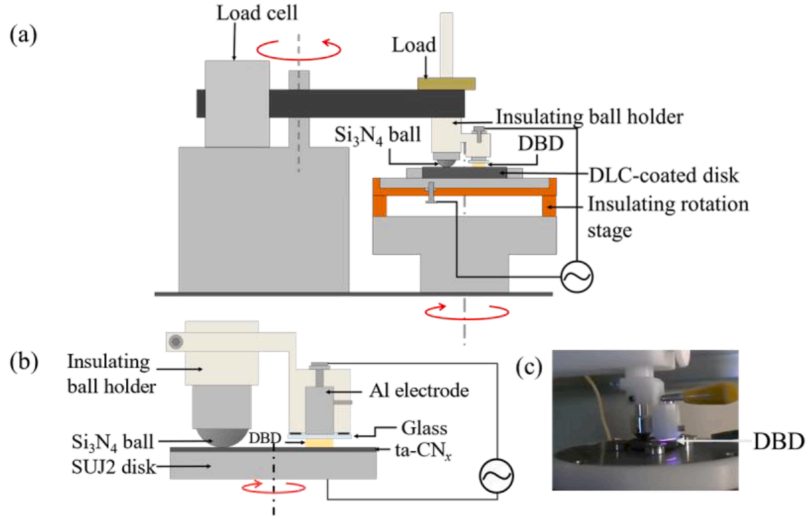

Fig. 2. (a) Schematic diagram of the ball-on-disk tribometer, (b) Enlarged view of the DBD part of the system, (c) Photographs of the DBD between the DLC-coated and glass plate-covered electrodes.

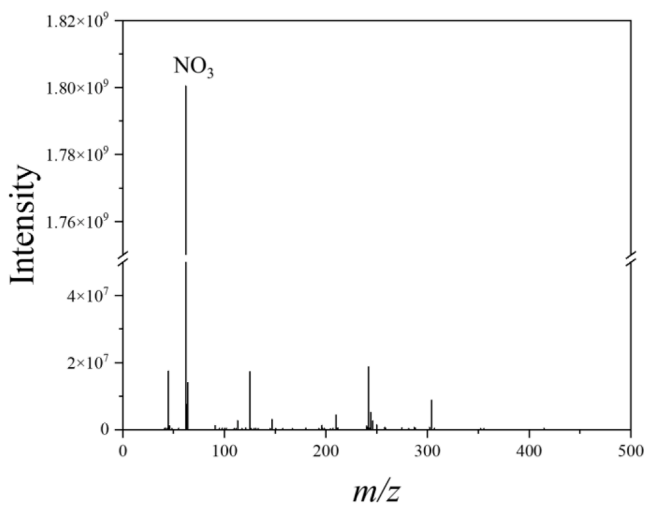

Fig. 3. LC-MS results of liquid film produced by DBD irradiation.

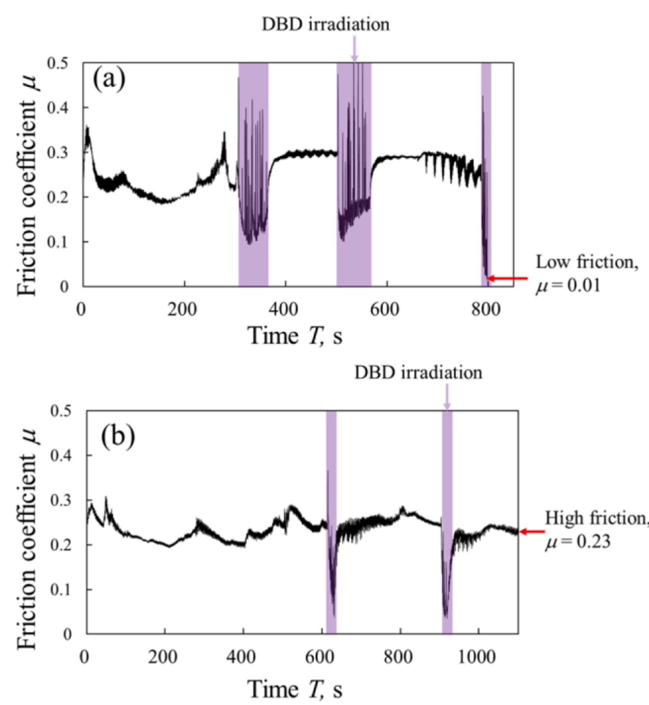

Fig. 4. Friction evolutions of *ta*-CN_x coatings: (a) When the friction coefficient reduced to 0.01 during *in situ* DBD irradiation, (b) When the friction coefficient increased to 0.23 after stopping DBD irradiation.

immediately to obtain a low friction sliding surface. To better explain the low friction mechanism, another friction test was conducted, as seen in Fig. 4b. The friction coefficient dropped significantly upon application of DBD irradiation, while it began to increase after stopping DBD irradiation, and finally, the sliding was halted when the friction coefficient increased to 0.23, a high friction surface was obtained. When DBD irradiation was stopped, the generation of the nitric acid-containing liquid film also ceased. Owing to the highly volatile nature of this liquid film, it evaporates rapidly within tens of seconds, leading to a quick dissipation of the liquid film. Consequently, the friction coefficient increased. Moreover, the friction coefficient gradually decreases with successive DBD irradiation cycles. These phenomena can be ascribed to the gradual alterations in surface chemical composition over time, as discussed in more detail below.

The laser microscopy images of the surface after different modes of DBD irradiation are shown in Fig. 5. The image of the *ta*-CN_x surface after DBD irradiation without any sliding test is seen in Fig. 5b. Compared with the as-deposited *ta*-CN_x coating (Fig. 5a), a lot of black material appeared due to merely DBD irradiation. The scattered distribution of black materials can be related to the characteristic of DBD discharge as filamentary discharge [39,40]. Fig. 5c shows the low friction image ($\mu = 0.01$) with *in situ* DBD irradiation. The surface shows at the edge of the wear track, a dark-colored tribofilm produced. In the same condition, a transfer layer has also appeared at the ball surface (Fig. 5d). Fig. 5e shows the high friction image ($\mu = 0.23$) after *in situ* DBD irradiation stopped. The dark-colored tribofilm at the wear track disappeared. Meanwhile, the transfer film on the ball surface disappeared due to friction (Fig. 5f). To better observe the changes in surface morphology, the DBD-irradiated *ta*-CN_x coating was examined using FE-SEM, as shown in Fig. 6. At a lower magnification (Fig. 6a), numerous bright spots are visible, which may represent the initial distribution of these sheet-like materials. As the magnification is increased (Fig. 6b and 6c), the sheet-like morphology becomes more apparent.

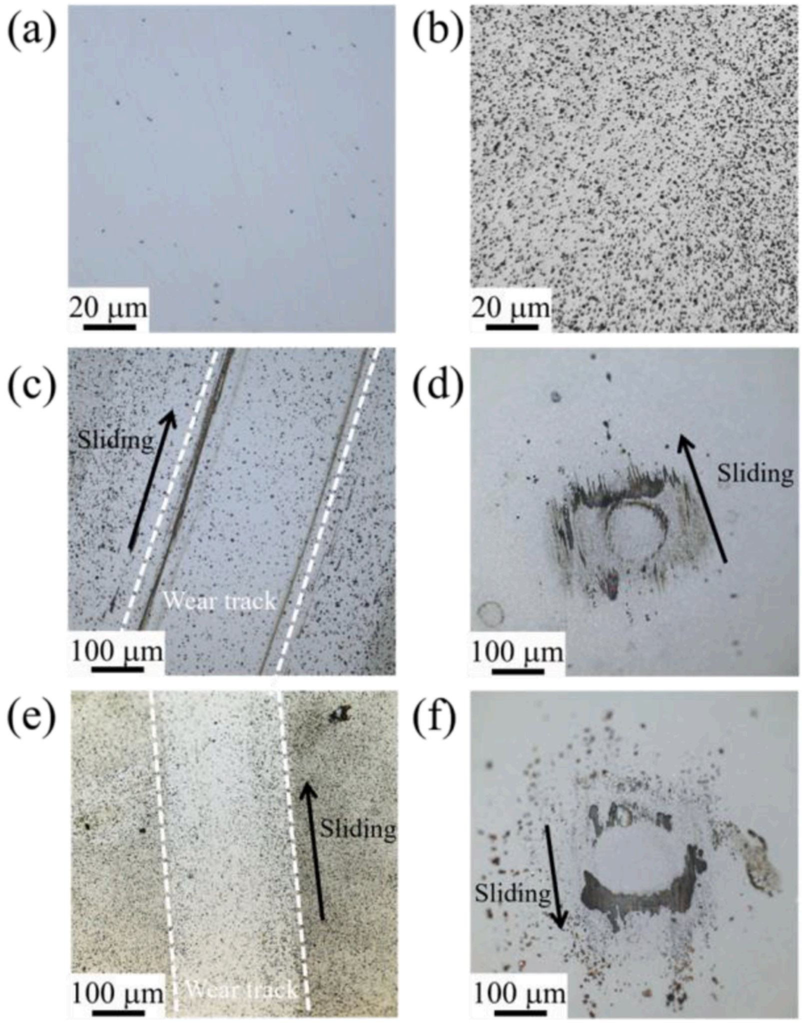

Fig. 5. Laser microscopy images of the *ta*-CN_x disk and ball specimens: (a) as-deposited *ta*-CN_x disk, (b) *ta*-CN_x disk after only DBD irradiation; (c) wear track when the friction coefficient reduced to 0.01 during *in situ* DBD irradiation, and (d) ball surface; (e) wear track when friction coefficient increased to 0.23 after stopping DBD irradiation, and (f) ball surface.

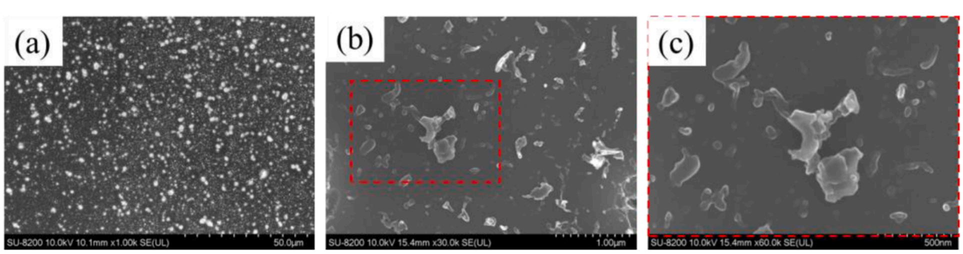

Fig. 6. FE-SEM images of the DBD-irradiated *ta*-CN_x coating surface. (a) 1000x, (b) 30000x, (c) 60000x.

3.3. Effect of DBD irradiation on the structure of ta-CN_x coating

To elucidate the impact of the transformation of carbonaceous film on the friction, Raman spectroscopy was performed. As shown in Fig. 7b, the black material produced by DBD irradiation exhibits different features compared to the as-deposited *ta*-CN_x coating (Fig. 7a): the D peak at 1348 cm^{-1} and the G peak at 1589 cm^{-1}. The D peak and G peak in the study of carbon-based materials provide information on the A_1g symmetric mode scattering due to structural defects, edge effects, or impurities (D peak) and the E_2g mode of carbon-carbon bond planar vibrations caused by sp^2 hybridized carbon atoms (G peak), respectively [41–43]. Some of the data shown in Fig. 7a and b, specifically the Raman spectra in the 800–2000 cm^{-1} range, were adapted from our conference proceedings [37]. These data were reused here as a baseline for further analysis and comparison. In this study, the analysis was extended to the 800–3200 cm^{-1} range, revealing additional structural features and providing deeper insights into the structural changes induced by DBD treatment. Broader 2D and D+D' peaks are observed in the 2400–3200 cm^{-1} range. They are caused by the two-phonon process. The appearance of the 2D peak usually indicates a certain degree of order or layered structure in the sp^2 carbon structure [44]. The characteristic of a graphite oxide structure is similar to the current Raman spectra. [45–47]. The Raman spectra of the *ta*-CN_x disk at the wear track with a reduced friction coefficient of 0.01 during *in situ* DBD irradiation are

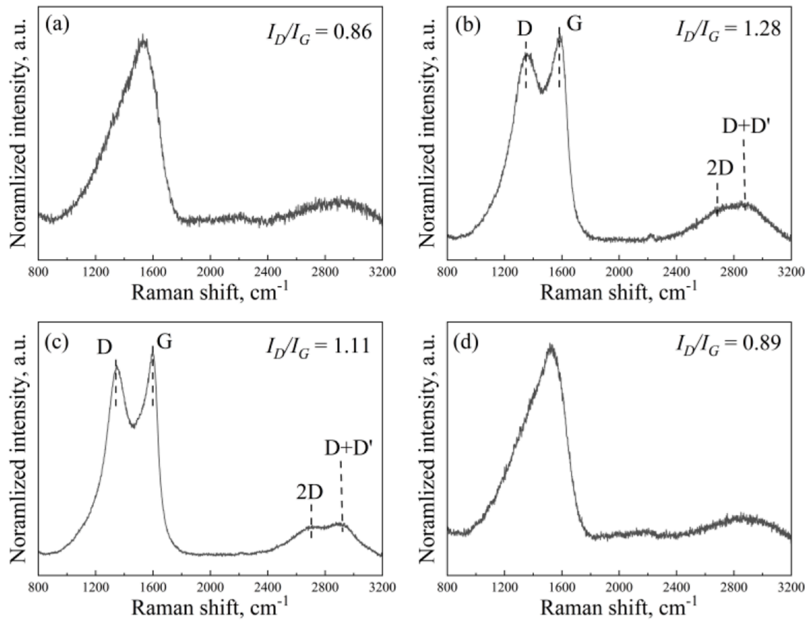

Fig. 7. Raman spectroscopy of *ta*-CN_x disk: (a) as-deposited *ta*-CN_x disk, (b) *ta*-CN_x disk after only DBD irradiation (the Raman spectra in the range of 800–2000 cm^{-1} were adapted from [37]), (c) the wear track of *ta*-CN_x disk when the friction coefficient reduced to 0.01 during *in situ* DBD irradiation, (d) the wear track of *ta*-CN_x disk when friction coefficient increased to 0.23 after stopping DBD irradiation.

displayed in Fig. 7c, the spectra also indicate that there are distinct D and G peaks, as well as a more clearly defined 2D peak. Fig. 7d shows the Raman spectra of the wear track with comparably high friction (μ = 0.23) after stopping DBD irradiation. From the figure, the Raman spectra of as-deposited *ta*-CN_x coating and the surface with increased friction coefficient are similar. To further understand the effect of DBD irradiation on the *ta*-CN_x coating, the spectra were used to calculate the I_D/I_G ratio and G peak position, which indicate the modification of the carbonaceous structures. Fig. 8 shows that the G peak position and I_D/I_G ratio increased for both the only DBD-irradiated surface and the low friction surface with *in situ* DBD irradiation compared to the as-deposited. Furthermore, many studies indicate that the graphitization of the carbonaceous structure of DLC coatings is responsible for this change. However, following the cessation of DBD irradiation, the G peak position and I_D/I_G ratio on the wear track both returned to their as-deposited coating values, and the friction coefficient increased to its initial level. These findings strongly suggest that DBD radiation speeds up the conversion of carbonaceous structures to sp^2-rich structures and that friction subsequently removes and transfers the majority of the sp^2-rich structures to the ball's surface. This corresponds to the findings of previous surface treatments mentioned in the literature [48].

To determine the detailed surface composition after DBD irradiation, the as-deposited *ta*-CN_x coatings and after DBD irradiation were analyzed by XAFS. Fig. 9 presents the C K-edge spectra. At photon energies over 290 eV, the XAFS spectra are mostly influenced by the 1s-σ* transition associated with carbon-carbon σ bonds [49,50]. A distinct characteristic peak is observed near 285.8 eV, representing the 1s-π* transition for the carbon-carbon bond [49,50]. Further comparison between the as-deposited *ta*-CN_x coating and DBD irradiated *ta*-CN_x coating revealed that two significantly different peaks A and B appeared in the DBD irradiated *ta*-CN_x coating. The A peak appears near 288.3 eV and is categorized as an oxygen functional group bonded to carbon,

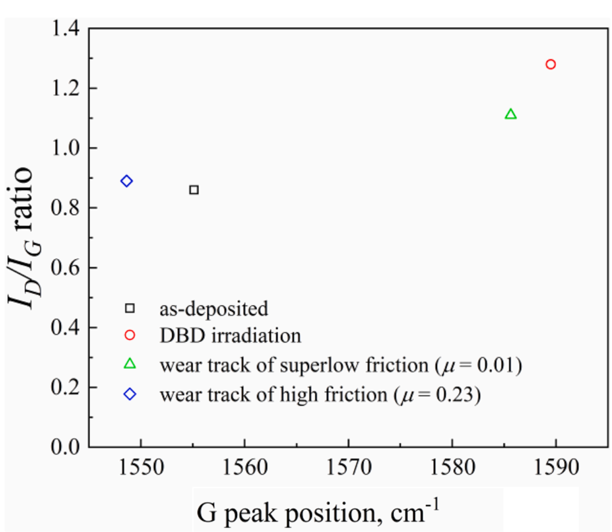

Fig. 8. G peak position and I_D/I_G ratio results of Raman analysis.

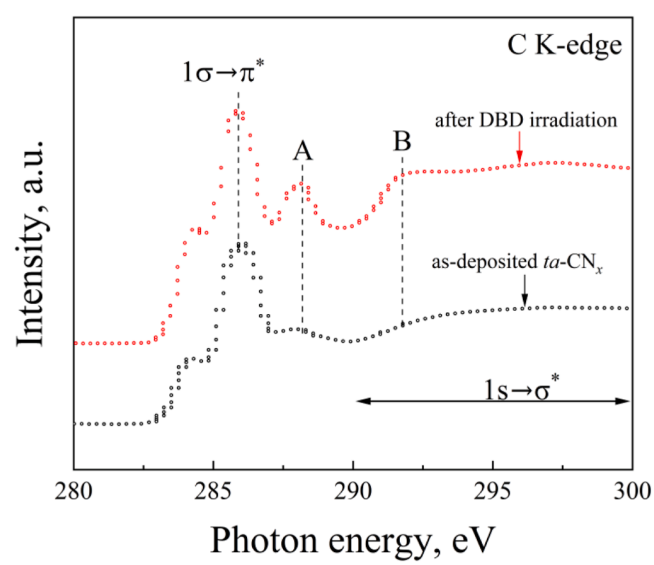

Fig. 9. C K-edge XAFS spectra of as-deposited *ta*-CN_x coating and *ta*-CN_x coating after DBD irradiation.

possibly corresponding to 1s-σ* (C-O) for the epoxy and hydroxyl groups, and 1s-σ* (C=O) for the carbonyl group [51,52]. The B peak appears at 291.7 eV, corresponding to the long-range order sp^2 [51]. The appearance of long-range order sp^2 peaks in the *ta*-CN_x coatings after DBD irradiation indicates a partial structural evolution of the material towards a graphitized or graphene-like structure. This corresponds to the findings of Raman analysis. The obtained results indicate the generation of oxygen functional groups bonded to carbon after DBD irradiation, as well as surface graphitization, possibly attributed to the generation of a graphite oxide structure.

3.4. Analysis of low friction surfaces ($\mu = 0.01$)

To better understand the superlow friction mechanism caused by DBD irradiation, surfaces that achieve low friction during DBD irradiation were selected for further analysis. The wear track was analyzed using XPS. Fig. 10a displays the survey spectra of the wear track with superlow friction and the as-deposited *ta*-CN_x. The O1 s peak appears at the wear track, and the N1 s peak intensity of as-deposited *ta*-CN_x coating is greater than that of the wear track. The atomic concentration was calculated using CasaXPS, which is shown in Fig. 10b. The N concentration was observed to decrease from 11.04 % to 5.15 %, indicating that certain amount of N atoms was involved in the nitric acid formation. Conversely, the O concentration increased from 0.28 to 7.61. This increase corresponds with the XAFS findings (Fig. 9) which demonstrate the generation of oxygen-containing functional groups after DBD irradiation. To reveal detailed bond configurations, the fine scans of the XPS spectra for C1 s, N1 s, and O1 s are shown in Fig. 11. For the as-deposited *ta*-CN_x coatings, the spectra corresponding to C1 s can be fitted to C=Csp^2 (284.6 eV), C-Csp^3 (285.5 eV), C=Nsp^2 (286.3 eV), C-Nsp^3 (287.5 eV), and C=O (288.6 eV). The peaks of N1 s can be fitted to C-Nsp^3 (398.6 eV), C=Nsp^2 (400.4 eV), and N-N/N-O (402.4 eV) [53–55], respectively. Compared to the as-deposited *ta*-CN_x coating, two different peaks appear in the C1 s peak: the C-O-C bond peak at 286.7 eV and the COOH bond peak at 288.9 eV [46]. For O1 s, three characteristic peaks corresponding to C=O (531.6 eV), C-OH (532.4 eV), and COOH (533.2 eV) appeared [56]. These results strongly indicate that oxygen-containing functional groups bonded to carbon at the wear track, achieving low friction during DBD irradiation. For the N1 s peak at the wear track (Fig. 11d), it can be fitted to pyridinic N (398.5 eV), pyrrolic N (400.1 eV), and graphitic N (401.2 eV) [57,58]. In addition, a shift of the peak at 402.4 eV to 402.9 eV was observed along with a significant narrowing of the FWHM. The shift in peak position and the decrease in FWHM usually indicate the formation of a more stable chemical bond between nitrogen and oxygen, especially the formation of pyridinic N oxides [58–61]. These findings indicate that the DBD treatment culminates in the formation of N-GO. The C-C sp^2/sp^3 ratio was determined, and the results showed that C-C sp^2/sp^3 at the wear track increased from 1.80 to 2.37 as compared to as-deposited *ta*-CN_x coating, which indicated that DBD irradiation and friction processes facilitated the conversion of sp^3 carbon to sp^2 carbon and formed more graphite-like structures. In summary, the obtained results strongly suggest that the realization of low friction is associated with the generation of N-GO.

3.5. Low friction mechanism due to DBD irradiation

As shown in Section 3.1, a liquid film containing nitric acid was generated on the surface when the DBD irradiated the *ta*-CN_x coating. In addition, the results from Sections 3.2 to 3.4 suggest the generation of N-GO structures due to DBD irradiation at the *ta*-CN_x interface. Consequently, it is hypothesized that the observed low friction results from a synergistic effect between N-GO and nitric acid. To verify the hypothesis, friction tests were conducted on DBD-irradiated *ta*-CN_x coatings with the addition of nitric acid. During the friction tests, nitric acid was incrementally added in three aliquots of 2 μl each. The friction coefficient initially recorded at 0.07 after the first addition, decreased to 0.02 after the third addition, as shown in Fig. 12. These findings support the hypothesis that the synergistic effect of nitric acid and N-GO substantially reduces the friction coefficient. Furthermore, to verify whether the low friction coefficient could be achieved by applying nitric acid directly, additional experiments were conducted where nitric acid was applied to the *ta*-CN_x surface without DBD irradiation. From the results, the average friction coefficient was 0.75. (Fig. 13), which, while lower than untreated surfaces, did not replicate the ultra-low friction observed with DBD irradiation. This suggests that DBD irradiation induces synergistic effects crucial for achieving ultra-low friction, particularly through the generation of N-GO structures. Therefore, the stability of the superlubricity state induced by DBD irradiation primarily based on the continuous formation and maintenance of the nitric acid-containing liquid film and formation of N-GO. Although liquid films are essential for reducing friction, their high volatility may affect the stability of the superlubricity state. Thus, additional research is necessary to gain a comprehensive understanding of the long-term stability of this superlubricity phenomenon. Previous studies revealed some low friction mechanisms. Li et al. demonstrated that the tribological characteristics of *a*-C coatings depend on the degree of surface graphitization, and ultra-low friction can be achieved for highly graphitized [62]. The realization of superlubrication of the *ta*-C tribopair in oleic acid was due to the tribochemical reaction that forms a graphene oxide structure [63]. Liu et al. demonstrated that graphene oxide can significantly lower the friction coefficient as a water-based lubricant additive [64]. There are also reports that ultra-low friction coefficients can be achieved by tailoring graphene additives or passivating *a*-C surfaces [65]. In addition, numerous studies have demonstrated the potential of graphite oxide (GO)-based materials as useful additives to reduce wear and friction in tribological systems. For example, Ge et al. demonstrated that the synergistic effect of GO nanoflakes and ethanediol could achieve

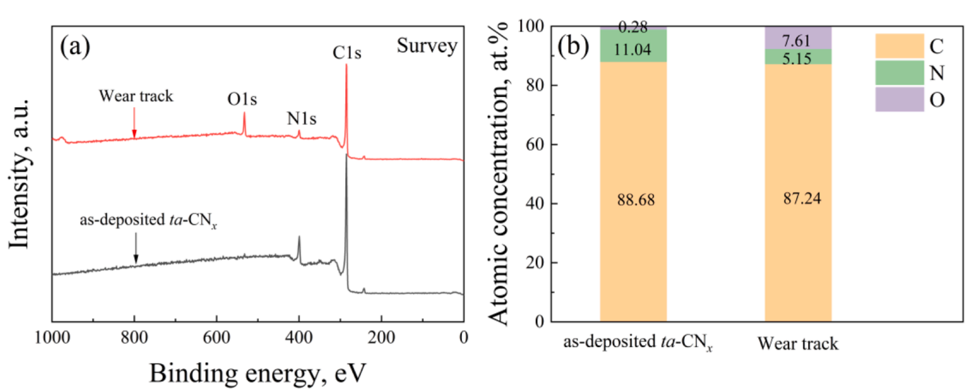

Fig. 10. (a) XPS survey spectra of the as-deposited *ta*-CN_x and the wear track, (b) Atomic concentration results.

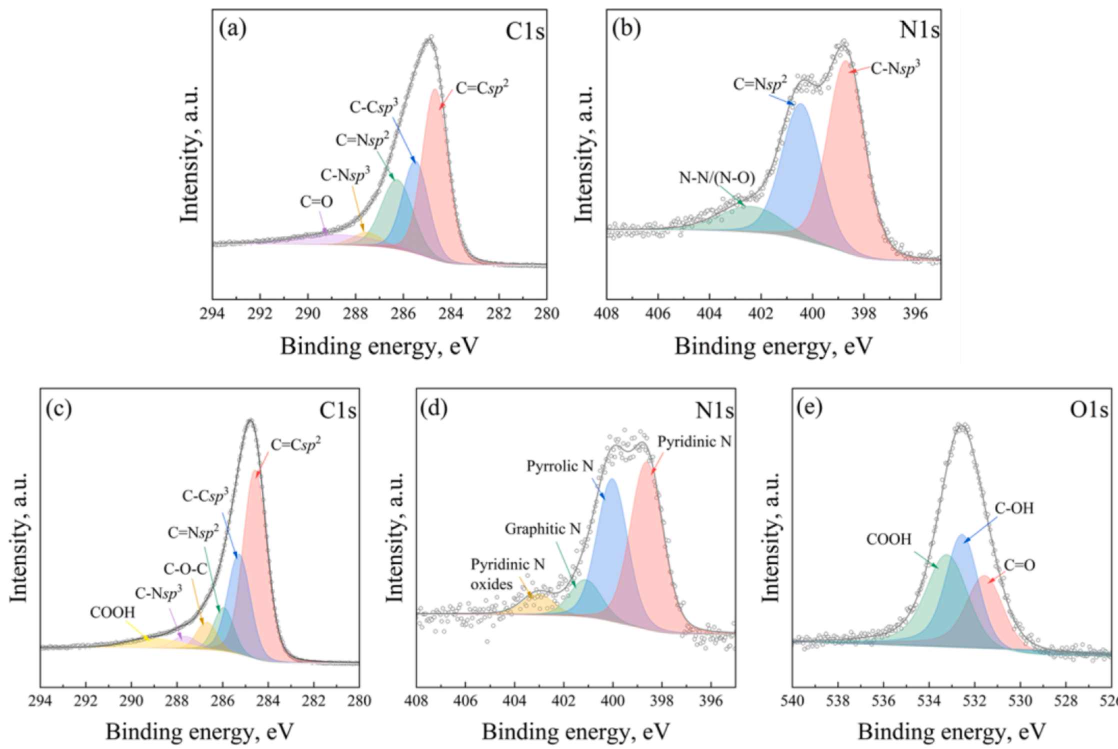

Fig. 11. XPS spectra of (a) C1 s and (b) N1 s of as-deposited *ta*-CN_x, (c) C1 s, (d) N1 s, and (e) O1 s of wear track.

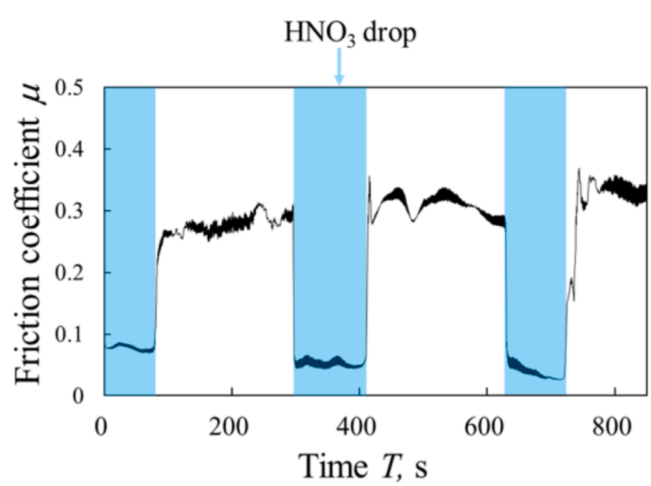

Fig. 12. Friction evolutions on DBD-irradiated *ta*-CN_x coatings with the addition of nitric acid.

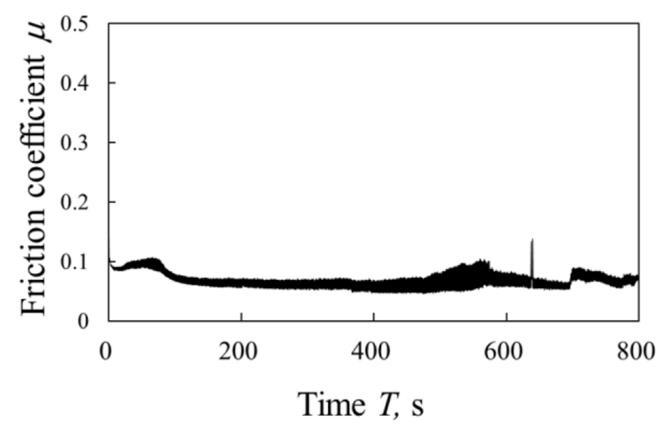

Fig. 13. Friction evolution of *ta*-CN_x coating without DBD irradiation after adding nitric acid.

superlubrication, highlighting GO's capability to significantly enhance lubrication performance under certain conditions [66]. Additionally, it has been reported that GO, when combined with ionic liquids, can achieve superlubrication under extreme pressures of up to 600 MPa, suggesting that GO can serve as a protective layer [67]. The tribological performance of GO is closely related to its degree of oxidation. For example, GO aqueous suspensions have demonstrated excellent friction-reducing capabilities, with performance strongly correlated with the oxidation level of GO [68]. Moreover, the pH of GO suspensions significantly influences their tribological properties. Acidic suspensions have been shown to greatly improve lubrication in steel ball/steel plate contacts, reducing the friction coefficient by 44.4 % compared to water [69,70]. In DLC/stainless steel contacts, GO water dispersions have been found to reduce the friction coefficient to 0.06 [71]. Furthermore, the low friction observed with GO and nanodiamonds in water-based lubricants are due to the generation of a friction-induced tribofilm, which facilitates sliding lubrication [72]. Compared to previous research [37], which highlighted the utility of DBD in reducing friction coefficients, our study delves more profoundly into the underlying mechanisms of these phenomena. These findings offer significant new insights into the tribological effects of DBD irradiation. While the reduction in friction on the *ta*-CN_x surface, facilitated by both nitric acid and N-GO, suggests a promising synergistic effect, the exact mechanisms (whether chemical, physical, or functional) remain to be fully established. Further investigations are needed to elucidate how these components interact at both molecular and surface levels.

This study proposes a low friction mechanism model for DBD irradiation of *ta*-CN_x coatings in ambient air (Fig. 14). The irradiation results in the formation of an acidic liquid film containing nitric acid on the *ta*-CN_x surface, as well as the development of oxygen-containing functional groups. During the DBD treatment, the surface of *ta*-CN_x is subjected to intense bombardment by high-energy particles such as ions

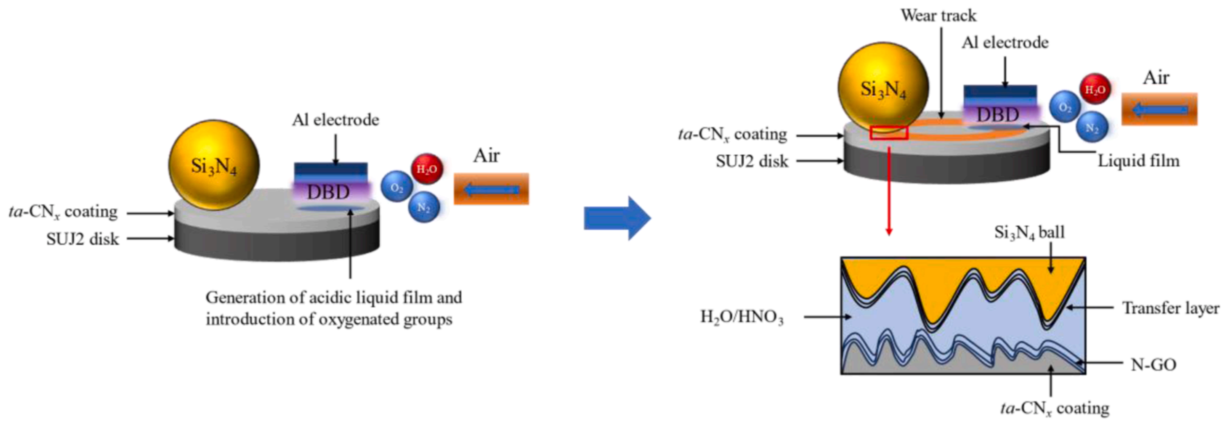

Fig. 14. Schematic of low friction mechanism.

and electrons. This bombardment disrupts the existing chemical bonds within the material, facilitating a transition from sp^3-hybridized carbon to sp^2-hybridized carbon. This transition leads to the graphitization of the surface and the generation of a N-GO structure. This structure further promotes the formation of a carbon-rich transfer film on the counter surface during the friction. Ultimately, low friction is achieved through the synergistic interaction of the N-GO layer, the liquid film containing nitric acid, and the transfer layer. This mechanism involves chemical modifications and changes in physical structure, as well as the cooperative action of lubricating layers, significantly reducing the friction coefficient. This novel low-friction mechanism provides important theoretical insights for the design and optimization of durable low-friction surface coatings.

4. Conclusion

This study explored the superlow friction mechanism in DBD-irradiated ta-CN_x coatings. The findings highlighted the role of an acidic liquid film containing nitric acid and the formation of N-GO in reducing friction. The synergistic interaction between these components under DBD irradiation led to effective lubrication in ambient air. The main conclusions were as follows:

(1) DBD irradiation generated an acidic liquid film on the ta-CN_x surface, confirmed to contain nitric acid.
(2) N-GO formation on the surface was verified through Raman, XAFS, and XPS analyses.
(3) The observed low friction resulted from the combined effects of N-GO and the nitric acid-containing liquid film.
(4) This mechanism allows for effective *in-situ* lubrication, enhancing the performance of ta-CN_x coatings.

CRediT authorship contribution statement

Wenjun Wu: Writing – original draft, Project administration, Methodology, Investigation, Data curation. **Motoyuki Murashima:** Writing – review & editing, Supervision, Methodology, Investigation, Formal analysis. **Noritsugu Umehara:** Writing – review & editing, Supervision, Methodology. **Takayuki Tokoroyama:** Writing – review & editing, Methodology. **Ruixi Zhang:** Writing – review & editing, Methodology.

Declaration of competing interest

The authors declare that they have no known competing financial interests or personal relationships that could have appeared to influence the work reported in this paper.

Acknowledgments

This work was financially supported by JST SPRING, Grant Number JPMJSP2125. The author (Wu)would like to take this opportunity to thank the “THERS Make New Standards Program for the Next Generation Researchers.”

This work was the result of using research equipment shared in MEXT Project for promoting public utilization of advanced research infrastructure (Program for supporting construction of core facilities) Grant Number JPMXS04411021.

Data availability

Data will be made available on request.

References

[1] K. Holmberg, A. Erdemir, Influence of tribology on global energy consumption, costs and emissions, Friction 5 (2017) 263–284, https://doi.org/10.1007/s40544-017-0183-5.
[2] K. Holmberg, P. Andersson, A. Erdemir, Global energy consumption due to friction in passenger cars, Tribol. Int. 47 (2011) 221–234, https://doi.org/10.1016/j.triboint.2011.11.022.
[3] J. Robertson, Diamond-like amorphous carbon, Mater. Sci. Eng. R Rep. 37 (2002) 129–281, https://doi.org/10.1016/S0927-796X(02)00005-0.
[4] A. Erdemir, Genesis of superlow friction and wear in diamondlike carbon films, Tribol. Int. 37 (2004) 1005–1012, https://doi.org/10.1016/j.triboint.2004.07.018.
[5] A. Erdemir, The role of hydrogen in tribological properties of diamond-like carbon films, Surf. Coat. Technol. 146–147 (2001) 292–297, https://doi.org/10.1016/S0257-8972(01)01417-7.
[6] G. Ma, S. Gong, G. Lin, L. Zhang, G. Sun, A study of structure and properties of Ti-doped DLC film by reactive magnetron sputtering with ion implantation, Appl. Surf. Sci. 258 (2012) 3045–3050, https://doi.org/10.1016/J.APSUSC.2011.11.034.
[7] D. Bootkul, B. Supsermpol, N. Saenphinit, C. Aramwit, S. Intarasiri, Nitrogen doping for adhesion improvement of DLC film deposited on Si substrate by filtered cathodic vacuum arc (FCVA) technique, Appl. Surf. Sci. 310 (2014) 284–292, https://doi.org/10.1016/J.APSUSC.2014.03.059.
[8] M. Murashima, X. Deng, H. Izuoka, N. Umehara, H. Kousaka, Effect of oxygen on degradation of defects on ta-C coatings deposited by filtered arc deposition, Surf. Coat. Technol. 362 (2019) 200–207, https://doi.org/10.1016/j.surfcoat.2019.01.115.
[9] J. Il Kim, Y.J. Jang, J. Kim, J. Kim, Effects of silicon doping on low-friction and high-hardness diamond-like carbon coating via filtered cathodic vacuum arc deposition, Sci. Rep. 11 (2021), https://doi.org/10.1038/s41598-021-83158-4.
[10] C. Kong, P. Guo, L. Sun, Y. Zhou, Y. Liang, X. Li, P. Ke, K.R. Lee, A. Wang, Tribological mechanism of diamond-like carbon films induced by Ti/Al co-doping, Surf. Coat. Technol. 342 (2018) 167–177, https://doi.org/10.1016/J.SURFCOAT.2018.02.098.
[11] W. Xu, K.S. Zhou, S. Lin, M. Dai, Q. Shi, C. Wei, Structural properties of hydrogenated Al-doped diamond-like carbon films fabricated by a hybrid plasma system, Diam. Relat. Mater. 87 (2018) 177–185, https://doi.org/10.1016/J.DIAMOND.2018.06.012.
[12] X. Liu, N. Umehara, T. Tokoroyama, M. Murashima, Tribological properties of ta-CNx coating sliding against steel and sapphire in unlubricated condition, Tribol. Int. 131 (2019) 102–111, https://doi.org/10.1016/J.TRIBOINT.2018.10.022.

[13] Y. Liu, X. Ge, J. Li, Graphene lubrication, Appl. Mater. Today 20 (2020), https://doi.org/10.1016/j.apmt.2020.100662.
[14] X. Ge, Z. Chai, Q. Shi, Y. Liu, W. Wang, Graphene superlubricity: a review, Friction 11 (2023) 1953–1973, https://doi.org/10.1007/s40544-022-0681-y.
[15] M. Guo, D. Diao, X. Fan, L. Yang, L. Yu, Scratch behavior of re-structured carbon coating by oxygen plasma etching technology for magnetic disk application, Surf. Coat. Technol. 251 (2014) 128–134, https://doi.org/10.1016/j.surfcoat.2014.04.014.
[16] C. López-Santos, M. Fernández-Gutiérrez, F. Yubero, B. Vazquez-Lasa, J. Cotrino, A. González-Elipe, J.S. Román, Effects of plasma surface treatments of diamond-like carbon and polymeric substrata on the cellular behavior of human fibroblasts, J. Biomater. Appl. 27 (2013) 669–683, https://doi.org/10.1177/0885328211422832.
[17] C. Jongwannasiri, S. Watanabe, Tribological behavior of O2 and CF4 plasma post-treated diamond-like carbon films under dry air and in a high relative humidity environment, Surf. Coat. Technol. 306 (2016) 200–204, https://doi.org/10.1016/j.surfcoat.2016.05.082.
[18] C. López-Santos, F. Yubero, J. Cotrino, A.R. González-Elipe, Lateral and in-depth distribution of functional groups on diamond-like carbon after oxygen plasma treatments, Diam. Relat. Mater. 20 (2011) 49–56, https://doi.org/10.1016/j.diamond.2010.11.024.
[19] J. Choi, S. Nakao, M. Ikeyama, T. Kato, Effect of oxygen plasma treatment on the tribological properties of Si-DLC coatings, Phys. Status Solidi (C) Curr. Top. Solid State Phys. 5 (2008) 956–959, https://doi.org/10.1002/pssc.200778302.
[20] D.Y. Yun, W.S. Choi, Y.S. Park, B. Hong, Effect of H 2 and O 2 plasma etching treatment on the surface of diamond-like carbon thin film, Appl. Surf. Sci. 254 (2008) 7925–7928, https://doi.org/10.1016/j.apsusc.2008.03.170.
[21] S.R. Polaki, N. Kumar, N. Gopala Krishna, T.R. Ravindran, M. Kamruddin, S. Dash, A.K. Tyagi, Tribological properties of chemically modified diamond like carbon films in hydrogen plasma, Tribol. Int. 81 (2015) 283–290, https://doi.org/10.1016/j.triboint.2014.09.009.
[22] M. Taufik Bin Taib, N. Umehara, T. Tokoroyama, M. Murashima, The effect of UV irradiation to a-C:h on friction and wear properties under PAO Oil lubrication including MoDTC and ZnDTP, Tribology 13 (2018) 119–130, https://doi.org/10.2474/trol.13.119.
[23] H. Tani, R. Naito, R. Lu, S. Koganezawa, N. Tagawa, Low Friction of diamond-like carbon film due to liquid hydrocarbon generated by laser heating in a nitrogen gas environment, 68 (2020) 88. 10.1007/s11249-020-01333-6.
[24] A.M. Khan, X. He, H. Wu, M. Desanker, A. Erdemir, Y.W. Chung, Q.J. Wang, Acid treatment of diamond-like carbon surfaces for enhanced adsorption of friction modifiers and friction performance, Tribol. Lett. 66 (2018), https://doi.org/10.1007/s11249-018-1081-3.
[25] J. Il Kim, Y.J. Jang, J. Kim, J.H. Jeong, Improvement of running-in process of tetrahedral amorphous carbon film sliding against Si3N4 under humid air by O2 plasma post-irradiation, Appl. Surf. Sci. 538 (2021), https://doi.org/10.1016/J.APSUSC.2020.147957.
[26] A. Lazauskas, M. Andrulevičius, B. Abakevičienė, D. Jucius, V. Grigaliūnas, A. Guobienė, Š. Meškinis, Hydrophilic surface modification of amorphous hydrogenated carbon nanocomposite films via atmospheric oxygen plasma treatment, Nanomaterials 13 (2023), https://doi.org/10.3390/nano13061108.
[27] H.E. Wagner, R. Brandenburg, K.V. Kozlov, A. Sonnenfeld, P. Michel, J.F. Behnke, The barrier discharge: basic properties and applications to surface treatment, Vacuum 71 (2003) 417–436, https://doi.org/10.1016/S0042-207X(02)00765-0.
[28] M. Nilkar, F.E. Ghodsi, S. Jafari, D. Thiry, R. Snyders, Effects of nitrogen incorporation on N-doped DLC thin film electrodes fabricated by dielectric barrier discharge plasma: structural evolution and electrochemical performances, J. Alloys Compd. 853 (2021), https://doi.org/10.1016/j.jallcom.2020.157298.
[29] T. Schuman, R.A. Wolf, Effects of a DBD plasma discharge on bond strength, Surfaces and Interfaces 18 (2020). 10.1016/j.surfin.2020.100461.
[30] K.G. Kostov, T.M.C. Nishime, L.R.O. Hein, A. Toth, Study of polypropylene surface modification by air dielectric barrier discharge operated at two different frequencies, Surf. Coat. Technol. 234 (2013) 60–66, https://doi.org/10.1016/j.surfcoat.2012.09.041.
[31] M. Murashima, K. Aono, N. Umehara, T. Tokoroyama, W.Y. Lee, Active control of lubricant flow using dielectrophoresis and its effect on friction reduction, Tribol. Online 18 (2023) 292–301, https://doi.org/10.2474/TROL.18.292.
[32] K. Suzuki, T. Ohzono, Wrinkles on a textile-embedded elastomer surface with highly variable friction, Soft Matter 12 (2016) 6176–6183, https://doi.org/10.1039/c6sm00728g.
[33] M. Murashima, S. Yoshino, M. Kawaguchi, N. Umehara, Intelligent tribological surfaces: from concept to realization using additive manufacturing, Int. J. Mech. Mater. Des. 15 (2019) 757–766, https://doi.org/10.1007/s10999-018-9435-4.
[34] M. Murashima, Y. Imaizumi, R. Murase, N. Umehara, T. Tokoroyama, T. Saito, M. Takeshima, Active friction control in lubrication condition using novel metal morphing surface, Tribol. Int. 156 (2021), https://doi.org/10.1016/j.triboint.2020.106827.
[35] M. Murashima, T. Yamada, N. Umehara, T. Tokoroyama, W.Y. Lee, Novel friction stabilization technology for surface damage conditions using machine learning, Tribol. Int. 180 (2023), https://doi.org/10.1016/j.triboint.2023.108280.
[36] W. Wu, M. Murashima, T. Saso, T. Tokoroyama, W.Y. Lee, H. Kousaka, N. Umehara, New *in situ* superlow-friction method for nitrogen-containing diamond-like carbon coatings using dielectric barrier discharge treatment in ambient air, Tribol. Int. 174 (2022), https://doi.org/10.1016/J.TRIBOINT.2022.107749.
[37] W. Wu, N. Umehara, T. Tokoroyama, M. Murashima, R. Zhang, Development of low-friction technology for treating nitrogen-containing diamond-like carbon coatings in ambient air using dielectric barrier discharge, in: E. Ciulli, A. Ruggiero (Eds.), Proceedings of the ITS-IFToMM 2024, Springer, Cham, 2024, pp. 99–106, https://doi.org/10.1007/978-3-031-62616-6_10.
[38] T. Shao, G. Wang, X. An, S. Zhuo, Y. Xia, C. Zhu, A reformative oxidation strategy using high concentration nitric acid for enhancing the emission performance of graphene quantum dots, RSC Adv. 4 (2014) 47977–47981, https://doi.org/10.1039/c4ra06935h.
[39] A. Chirokov, A. Gutsol, A. Fridman, Atmospheric pressure plasma of dielectric barrier discharges, Pure Appl. Chem. 77 (2005) 487–495, https://doi.org/10.1351/pac200577020487.
[40] J. Li, C. Ma, S. Zhu, F. Yu, B. Dai, D. Yang, A review of recent advances of dielectric barrier discharge plasma in catalysis, Nanomaterials 9 (2019), https://doi.org/10.3390/nano9101428.
[41] W.G. Cui, Q.B. Lai, L. Zhang, F.M. Wang, Quantitative measurements of sp3 content in DLC films with Raman spectroscopy, Surf. Coat. Technol. 205 (2010) 1995–1999, https://doi.org/10.1016/j.surfcoat.2010.08.093.
[42] M. Ayiania, E. Weiss-Hortala, M. Smith, J.S. McEwen, M. Garcia-Perez, Microstructural analysis of nitrogen-doped char by Raman spectroscopy: raman shift analysis from first principles, Carbon 167 (2020) 559–574, https://doi.org/10.1016/j.carbon.2020.05.055. N. Y.
[43] A.C. Ferrari, S.E. Rodil, J. Robertson, Resonant Raman spectra of amorphous carbon nitrides: the G peak dispersion, Diam. Relat. Mater. 12 (2003) 905–910, https://doi.org/10.1016/S0925-9635(02)00370-9.
[44] A. Merlen, J.G. Buijnsters, C. Pardanaud, A guide to and review of the use of multiwavelength Raman spectroscopy for characterizing defective aromatic carbon solids: from graphene to amorphous carbons, Coatings 7 (2017), https://doi.org/10.3390/coatings7100153.
[45] B. Ma, R.D. Rodriguez, A. Ruban, S. Pavlov, E. Sheremet, The correlation between electrical conductivity and second-order Raman modes of laser-reduced graphene oxide, Phys. Chem. Chem. Phys. 21 (2019) 10125–10134, https://doi.org/10.1039/c9cp00093c.
[46] F. Yin, S. Wu, Y. Wang, L. Wu, P. Yuan, X. Wang, Self-assembly of mildly reduced graphene oxide monolayer for enhanced Raman scattering, J. Solid State Chem. 237 (2016) 57–63, https://doi.org/10.1016/j.jssc.2016.01.015.
[47] E. Sujiono, D. Zabrian, M. Dahlan, B. Amin, J. Agus, Graphene oxide based coconut shell waste: synthesis by modified Hummers method and characterization, Heliyon 6 (2020), https://doi.org/10.1016/j.heliyon.2020.e04568.
[48] M. Murashima, S. Oyama, H. Kousaka, T. Tokoroyama, W.Y. Lee, N. Umehara, New *in situ* low-friction technology for diamond-like carbon coatings using surface discharge treatment in ambient air, Tribol. Int. 165 (2022), https://doi.org/10.1016/j.triboint.2021.107306.
[49] Z. Li, J.Z. Ye, J. Yan, N. Molina, H.M. Lien, R. Chrostowksi, C. Jaye, D.A. Fischer, J. Lin, F. Mangolini, Effect of tribologically-induced changes in surface termination of silicon-containing diamond-like carbon coatings on the resistance to biomolecule adsorption, Carbon. N. Y. 199 (2022) 132–140, https://doi.org/10.1016/j.carbon.2022.07.043.
[50] S.E. Rodil, S. Muhl, Bonding in amorphous carbon nitride, Diam. Relat. Mater. 13 (2004) 1521–1531, https://doi.org/10.1016/j.diamond.2003.11.008.
[51] S. Sainio, N. Wester, A. Aarva, C.J. Titus, D. Nordlund, E.I. Kauppinen, E. Leppänen, T. Palomäki, J.E. Koehne, O. Pitkänen, K. Kordas, M. Kim, H. Lipsanen, M. Mozetič, M.A. Caro, M. Meyyappan, J. Koskinen, T. Laurila, Trends in carbon, oxygen, and nitrogen core in the X-ray absorption spectroscopy of carbon nanomaterials: a guide for the perplexed, J. Phys. Chem. C 125 (2021) 973–988, https://doi.org/10.1021/acs.jpcc.0c08597.
[52] J. Etula, N. Wester, T. Liljeström, S. Sainio, T. Palomäki, K. Arstila, T. Sajavaara, J. Koskinen, M.A. Caro, T. Laurila, What determines the electrochemical properties of nitrogenated amorphous carbon thin films?, Cite this, Chem. Mater. 33 (2021) 6813–6824, https://doi.org/10.1021/acs.chemmater.1c01519.
[53] R. McCann, S.S. Roy, P. Papakonstantinou, M.F. Bain, H.S. Gamble, J. A. McLaughlin, Chemical bonding modifications of tetrahedral amorphous carbon and nitrogenated tetrahedral amorphous carbon films induced by rapid thermal annealing, Thin Solid Films 482 (2005) 34–40, https://doi.org/10.1016/j.tsf.2004.11.151.
[54] J. Corona-Gomez, S. Shiri, M. Mohammadtaheri, Q. Yang, Adhesion enhancement of DLC on CoCrMo alloy by diamond and nitrogen incorporation for wear resistant applications, Surf. Coat. Technol. 332 (2017) 120–127, https://doi.org/10.1016/j.surfcoat.2017.10.050.
[55] J. Peng, J. Huang, Y. Peng, Y. Xiao, M. Yang, Investigating the effect of bias voltage on the microstructural thermal stability and tribological performance of N-doped hydrogenated diamond-like carbon coatings, Surf. Coat. Technol. 451 (2022), https://doi.org/10.1016/j.surfcoat.2022.129064.
[56] C.H. Chuang, S.C. Ray, D. Mazumder, S. Sharma, A. Ganguly, P. Papakonstantinou, J.W. Chiou, H.M. Tsai, H.W. Shiu, C.H. Chen, H.J. Lin, J. Guo, W.F. Pong, Chemical modification of graphene oxide by nitrogenation: an X-ray absorption and emission spectroscopy study, Sci. Rep. 7 (2017), https://doi.org/10.1038/srep42235.
[57] K. Akada, S. Obata, K. Saiki, Radio-frequency plasma assisted reduction and nitrogen doping of graphene oxide, Carbon 189 (2022) 571–578, https://doi.org/10.1016/j.carbon.2021.12.074. N. Y.
[58] H. Wang, T. Maiyalagan, X. Wang, Review on recent progress in nitrogen-doped graphene: synthesis, characterization, and its potential applications, ACS Catal. 2 (2012) 781–794, https://doi.org/10.1021/cs200652y.
[59] J. Li, X. Li, P. Zhao, D.Y. Lei, W. Li, J. Bai, Z. Ren, X. Xu, Searching for magnetism in pyrrolic N-doped graphene synthesized via hydrothermal reaction, Carbon 84 (2015) 460–468, https://doi.org/10.1016/j.carbon.2014.12.024. N. Y.
[60] D. Long, W. Li, L. Ling, J. Miyawaki, I. Mochida, S.H. Yoon, Preparation of nitrogen-doped graphene sheets by a combined chemical and hydrothermal

reduction of graphene oxide, Langmuir 26 (2010) 16096–16102, https://doi.org/10.1021/la102425a.

[61] Y. Shao, S. Zhang, M.H. Engelhard, G. Li, G. Shao, Y. Wang, J. Liu, I.A. Aksay, Y. Lin, Nitrogen-doped graphene and its electrochemical applications, J. Mater. Chem. 20 (2010) 7491–7496, https://doi.org/10.1039/c0jm00782j.

[62] X. Li, N. Du, C. Feng, K. Chen, X. Wei, D. Zhang, K.R. Lee, Theoretical superlubricity and its friction stability of amorphous carbon film induced by simple surface graphitization, Appl. Surf. Sci. 615 (2023), https://doi.org/10.1016/j.apsusc.2022.156318.

[63] M.I. De Barros Bouchet, J.M. Martin, J. Avila, M. Kano, K. Yoshida, T. Tsuruda, S. Bai, Y. Higuchi, N. Ozawa, M. Kubo, M.C. Asensio, Diamond-like carbon coating under oleic acid lubrication: evidence for graphene oxide formation in superlow friction, Sci. Rep. 7 (2017), https://doi.org/10.1038/srep46394.

[64] Y. Liu, S. Yu, Z. Fan, X. Ge, W. Wang, How does lateral size influence the tribological behaviors of graphene oxide as nanoadditive for water-based lubrication? Carbon (2024) 219, https://doi.org/10.1016/j.carbon.2024.118803. N. Y.

[65] X. Li, D. Zhang, X. Xu, K.R. Lee, Tailoring the nanostructure of graphene as an oil-based additive: toward synergistic lubrication with an amorphous carbon film, ACS Appl. Mater. Interfaces 12 (2020) 43320–43330, https://doi.org/10.1021/acsami.0c12890.

[66] X. Ge, J. Li, R. Luo, C. Zhang, J. Luo, Macroscale superlubricity enabled by the synergy effect of graphene-oxide nanoflakes and ethanediol, ACS. Appl. Mater. Interfaces 10 (2018) 40863–40870, https://doi.org/10.1021/acsami.8b14791.

[67] X. Ge, J. Li, H. Wang, C. Zhang, Y. Liu, J. Luo, Macroscale superlubricity under extreme pressure enabled by the combination of graphene-oxide nanosheets with ionic liquid, Carbon 151 (2019) 76–83, https://doi.org/10.1016/j.carbon.2019.05.070. N. Y.

[68] L. Zhao, H. Yang, C. Liu, S. Xue, Z. Deng, J. Li, X. Zeng, The correlation between molecular structure and tribological properties of graphene oxide with different oxidation degree, Tribol. Lett. 67 (2019), https://doi.org/10.1007/s11249-019-1199-y.

[69] A.A. Alias, H. Kinoshita, Y. Nishina, M. Fujii, Dependence of ph level on tribological effect of graphene oxide as an additive in water lubrication, Int. J. Automot. Mech. Eng. 13 (2016) 3150–3156, https://doi.org/10.15282/ijame.13.1.2016.2.0262.

[70] A. He, S. Huang, J.H. Yun, Z. Jiang, J. Stokes, S. Jiao, L. Wang, H. Huang, The pH-dependent structural and tribological behaviour of aqueous graphene oxide suspensions, Tribol. Int. 116 (2017) 460–469, https://doi.org/10.1016/j.triboint.2017.08.008.

[71] O. Elomaa, V.K. Singh, A. Iyer, T.J. Hakala, J. Koskinen, Graphene oxide in water lubrication on diamond-like carbon vs. stainless steel high-load contacts, Diam. Relat. Mater. 52 (2015) 43–48, https://doi.org/10.1016/j.diamond.2014.12.003.

[72] P. Wu, X. Chen, C. Zhang, J. Luo, Synergistic tribological behaviors of graphene oxide and nanodiamond as lubricating additives in water, Tribol. Int. 132 (2019) 177–184, https://doi.org/10.1016/j.triboint.2018.12.021.